WIDEBAND HIGH EFFICIENCY OPTICAL MODULATOR

Final Report

15 February 1966 to 15 March 1967

Contract No. NAS 8-20545

by

W. J. Rattman
B. K. Yap
W. E. Bicknell

Submitted to

NATIONAL AERONAUTICS AND SPACE ADMINISTRATION
GEORGE C. MARSHALL SPACE FLIGHT CENTER
HUNTSVILLE, ALABAMA 35812

APPLIED RESEARCH LABORATORY
SYLVANIA ELECTRONIC SYSTEMS
A Division of Sylvania Electric Products Inc.
40 Sylvan Road, Waltham, Massachusetts 02154

WIDEBAND HIGH EFFICIENCY OPTICAL MODULATOR

Final Report

15 February 1966 to 15 March 1967

Contract No. NAS 8-20545

by

W. J. Rattman
B. K. Yap
W. E. Bicknell

Submitted to

NATIONAL AERONAUTICS AND SPACE ADMINISTRATION
GEORGE C. MARSHALL SPACE FLIGHT CENTER
HUNTSVILLE, ALABAMA 35812

APPLIED RESEARCH LABORATORY
SYLVANIA ELECTRONIC SYSTEMS
A Division of Sylvania Electric Products Inc.
40 Sylvan Road, Waltham, Massachusetts 02154

ABSTRACT

This is the final report of a project to develop two 100-MHz bandwidth electro-optic modulators and solid-state drivers which achieve 100 percent amplitude modulation with less than 10 watts modulator drive power. This report treats the design of this optical modulation system and the results of tests performed over the full 100-MHz bandwidth.

TABLE OF CONTENTS

Section		Page
1	INTRODUCTION	1-1
2	MODULATOR DESIGN CONSIDERATIONS	2-1
	2.1 MODULATOR CELL	2-3
	2.1.1 Video Drive Power	2-3
	2.1.2 Modulator Bandwidth	2-6
	2.2 BEAM CONDENSER	2-9
	2.3 CRYSTAL SURFACE QUALITY	2-13
3	SOLID-STATE DRIVER DESIGN	3-1
4	EXPERIMENTAL	4-1
	4.1 LOW FREQUENCY TESTS	4-1
	4.1.1 Extinction Ratio	4-1
	4.1.2 Thermal Stability	4-1
	4.2 OPTICAL EFFICIENCY	4-1
	4.3 SYSTEM OPERATION OVER 100-MHz BANDWIDTH	4-4
	4.3.1 Direct Detection	4-4
	4.3.2 Modulation Measurements by DC Shift Method	4-4
	4.4 MODULATOR SYSTEM PULSE PERFORMANCE	4-9
	4.5 DESIGN AND TEST DATA SUMMARY	4-12
5	CONCLUSIONS	5-1
6	REFERENCES	6-1
Appendix		
A	EXPERIMENTAL TEST MODULATORS	A-1
B	20 WATT TRANSISTORIZED DISTRIBUTED AMPLIFIER	B-1

LIST OF ILLUSTRATIONS

Figure		Page
1-1	KD*P Modulator	1-2
2-1	Modulator Internal View	2-2
2-2	Modulator Length vs. Beam Reduction Factor	2-12
2-3	Crystal Surface Imperfections	2-14
2-4	KDA Optical Surface Micrographs	2-15
3-1	100 MHz Video Amplifier	3-2
3-2	Preamplifier Schematic	3-3
3-3	Power Amplifier Schematic	3-4
3-4	100 MHz Video Amplifier Response	3-6
4-1	KD*P Modulator 25:1 Extinction Ratio	4-2
4-2	Percent Modulation vs. Frequency	4-5
4-3	Modulation Measurement: DC Shift Method	4-6
4-4	Modulator Pulse Response	4-10
4-5	Modulator System Pulse Response	4-11
A-1	Test Modulator	A-2
A-2	KDA Modulator Operation at 10 MHz	A-3
A-3	LN Optical Surface Micrographs	A-5
B-1	20 Watt Transistorized Distributed Amplifier	B-2

LIST OF TABLES

Number		Page
2-1	Alternate 10-Watt, 100-MHz Video Modulators	2-7
4-1	Modulator Optical Efficiency	4-3
4-2	KD*P Modulator Summary	4-12
A-1	KDA Test Modulator Summary	A-4
A-2	LN Test Modulator Summary	A-6
A-3	Electro-Optic Crystal Constants	A-8

SECTION 1

INTRODUCTION

Interest in mechanizing optical modulation systems with wide instantaneous bandwidths has been stimulated by present-day multiple-frequency ranging system requirements and by future communication system requirements. The principal shortcoming of the electro-optic modulator was its need for large drive power levels when operated over wide bandwidths. For instance, the S2A, an optical intensity modulator developed by this laboratory, required up to 500-volts rms and 270 watts nominally for operation over a 50-MHz video bandwidth.

The goals of this contract were to develop an optical modulator and transistorized driver comprising a modulation system operable over a 100-MHz video bandwidth with less than 10-watts modulator drive power. The solution to this modulator design problem was achieved by combining small cross-section potassium dideuterium phosphate (KD*P) crystals with laser beam-condensing optics. Modulator length was held to an absolute minimum to preserve optical performance comparable to that of the S2A.

Two modulators (Figure 1-1) and solid-state drivers were delivered that achieved 100 percent optical intensity modulation with 6 watts drive power to the modulator over an instantaneous 100-kHz to 100-MHz bandwidth. This development indicates the feasibility of future space wide-band communication systems. This report treats the design of this optical modulation system and the results of tests performed over the 100-MHz band.

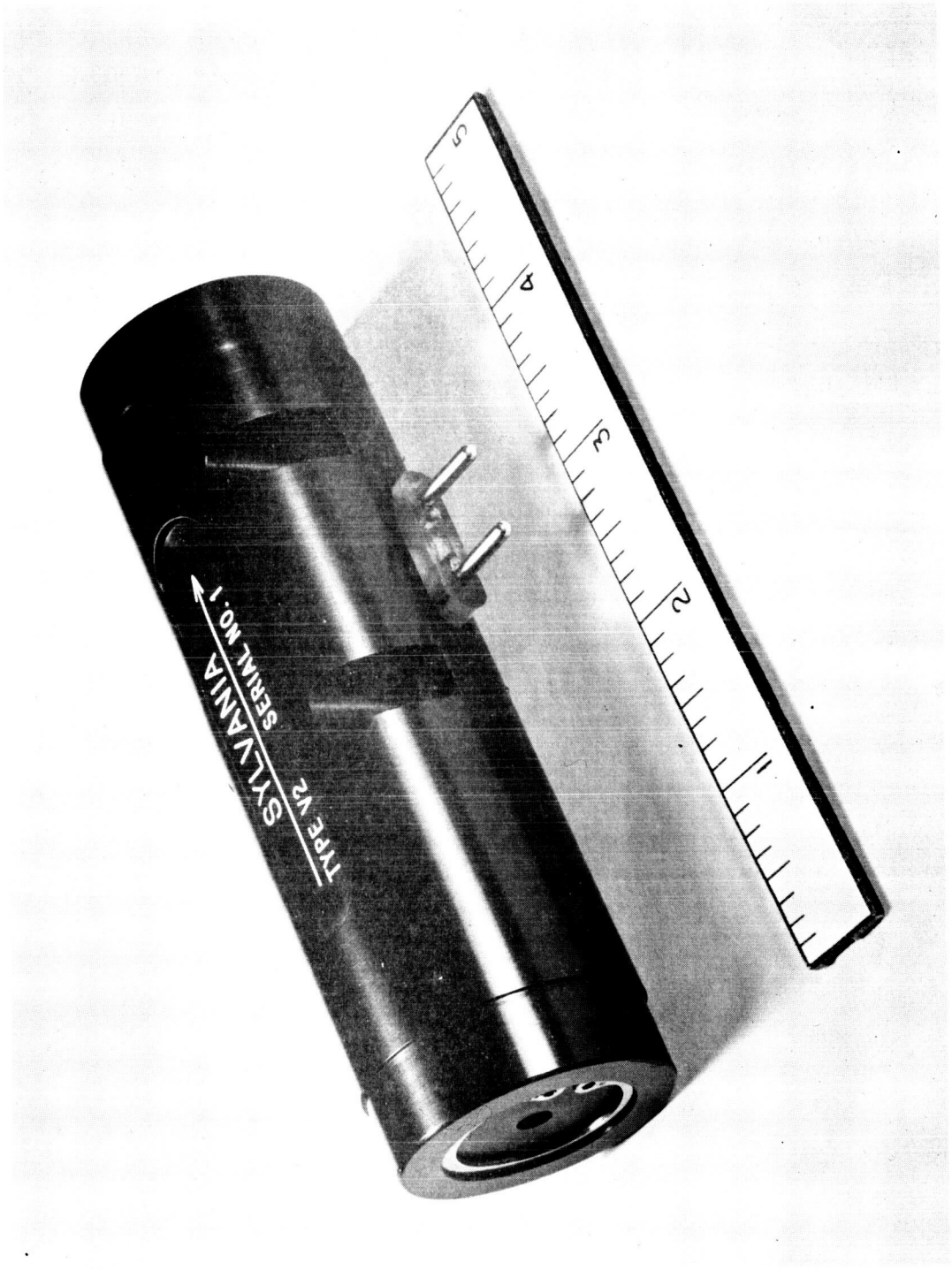

Figure 1-1. KD*P Modulator

SECTION 2

MODULATOR DESIGN CONSIDERATIONS

Experimental small cross-section modulators were constructed during the early phase of this program and operated over the 100-MHz video bandwidth. These test modulators employed potassium dihydrogen arsenate (KDA) and lithium niobate (LN) crystals of 1-mm cross section in balanced cells with aspect ratios of 40; i.e., with a modulator cell length to height ratio of 40 mm: 1 mm. The attainment of a 16:1 optical intensity extinction ratio and the detection of modulation over the 100-MHz band with the KDA prototype device proved the feasibility of a lumped-element transverse modulator design combined with beam forming optics to meet the 10-watt drive power requirement. The LN device demonstrated poor optical performance and exhibited internal crystal inhomogeneities as found by other investigators.[1,2] Detailed test results for both experimental modulators appear in Appendix A.

The internal view (Figure 2-1) shows construction details of the transverse lumped-element electro-optical modulator. A laser beam-condenser is employed at the modulator input to reduce and collimate the beam. The now classical balanced construction of the modulator cell employs equal length crystals on each side of a half-wave plate with their optic axes opposite in sense to balance the natural birefringence of the electro-optic element that is a function of temperature. When a voltage is applied across the cell, generating an E field along the optical (Z) axis of the crystals, a phase retardation is imparted to the x component of a light beam propagating along the y axis. The retardation is given in terms of the electro-optic material parameters by:

$$\phi = \frac{\pi \eta_o^3 r_{63}}{\lambda} \frac{\ell V}{b} \qquad (1)$$

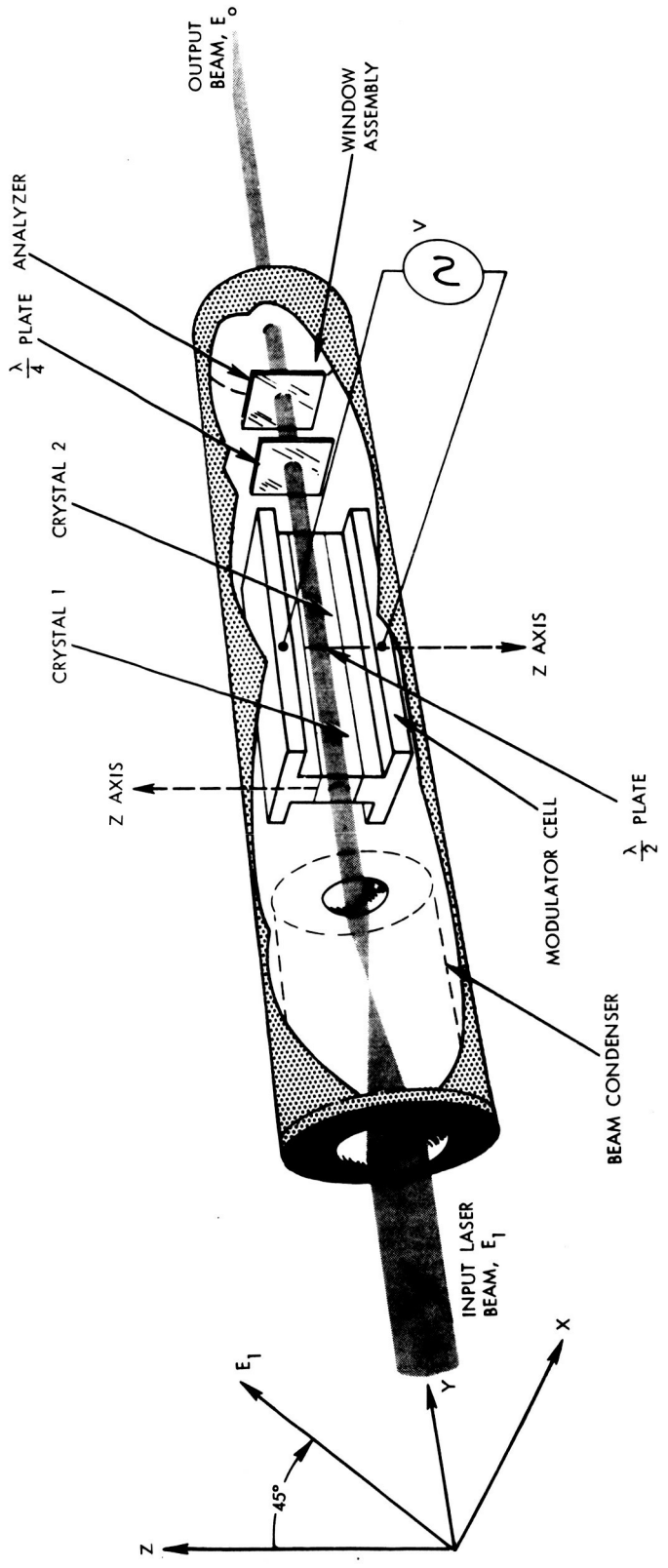

Figure 2-1. Modulator Internal View

where

ϕ = phase retardation in radians

η_o = ordinary index of refraction

r_{63} = electro-optic coefficient in meters/volt

λ = wavelength of optical carrier in meters

ℓ = modulator cell length

V = applied voltage

b = dimension of the crystal across which voltage is applied.

The result of the retardation imparted to the x component of the light beam is a conversion of linearly polarized input light to an elliptically polarized output. The analyzer in the output window converts the polarization modulated beam to intensity modulation. The quarter-wave plate biases the system to align the peak-modulated polarization vector with the analyzer axis, thus eliminating the need for a dc bias component in the applied modulation voltage.

2.1 MODULATOR CELL

2.1.1 Video Drive Power

The drive voltage requirement for the transverse modulator is determined by the half-wave field-distance product of the electro-optic element and its aspect ratio (length to height ratio) according to:[4]

$$V_\pi = \frac{\{E \cdot \ell\}_{\lambda/2}}{\ell/b} \qquad (2)$$

where

V_π = the peak-to-peak drive voltage required for operation to extinction

b = the crystal height in the direction of the applied electric field

ℓ = the crystal length in contact with the electrodes

ℓ/b = the aspect ratio, and

$\left\{E\cdot\ell\right\}_{\lambda/2}$ = the half-wave retardation voltage for the crystal material, otherwise known as the half-wave field-distance product.

For comparison of drive power-bandwidth requirements for the modulator cell designs considered during this program, it is more convenient to use rms values. For this purpose we write

$$V = \frac{V_\pi}{2\sqrt{2}} = M\,\frac{b}{\ell} \tag{3}$$

where V is the rms drive voltage required for operation to extinction, and

$$M = \frac{\left\{E\cdot\ell\right\}_{\lambda/2}}{2\sqrt{2}} \tag{4}$$

The peak-to-peak half-wave retardation voltage is given by:

$$\left\{E\cdot\ell\right\}_{\lambda/2} = \frac{\lambda}{\eta_o^3 r_{63}} \tag{5}$$

where

λ = optical wavelength

η_o = ordinary index of refraction

r_{63} = electro-optic coefficient.

For modulation frequencies up to several hundred megahertz, the length of video modulator crystal assemblies considered here is less than the modulation frequency wavelength, consequently the crystal and electrode structure may be regarded simply as a capacitor. Modulator capacitance equals crystal

and stray capacitance. During this work, stray capacitance was minimized. The modulator crystal capacitance for crystals of square cross section is given by:

$$c = K\epsilon_o \ell \tag{6}$$

where

K = crystal relative dielectric constant

ϵ_o = permittivity of free space (8.85 pF/m).

The modulator capacitance and the desired operating bandwidth place a limit on a driver shunting resistance according to:

$$R \leq \frac{1}{2\pi f_2 K\epsilon_o \ell} \tag{7}$$

This requires that the driver be capable of delivering power over the video band to the shunting resistance. For 100 percent modulation over the bandwidth, f_2, that power becomes:

$$P = \frac{M^2 b^2 \cdot 2\pi f_2 K\epsilon_o}{\ell} \tag{8}$$

Broadbanding techniques are often used to achieve bandwidth improvements of, typically, 1.8 to 3.5.[3] Double pi filter networks employed in the video amplifiers developed under this contract achieved bandwidth improvement of 3.5 when the total modulator capacitance and connecting cable capacitance were included. Broadbanding techniques will allow for a corresponding drive power reduction for a given bandwidth as given by:

$$P = \frac{M^2 b^2 2\pi f_2 \cdot K\epsilon_o}{3.5\ell} \tag{9}$$

Rearranging Eq. (9) and combining constants, we obtain the expression for drive power per megahertz of bandwidth for a modulator with zero stray capacitance:

$$P' = \frac{15.9\left(10^{-6}\right)M^2 b^2 K}{\ell} (\text{watts/MHz}) \qquad (10)$$

Practical considerations must take account of modulator stray capacitance and that of connecting leads to the driver's terminating resistance. This is easily done by modifying K to take these effects into account. The KD*P modulators developed under this contract, considering stray as well as connecting capacitances, achieved a 60 mW/MHz drive power requirement.

Before deciding upon KD*P as the electro-optic element for the 100-MHz modulators, several materials were considered.[4] The design values for transverse modulator designs using these materials are given in Table 2-1. The design constraint is a 10-watt maximum drive power requirement using a bandwidth improvement factor of 1.8. The advantages afforded by the 3/4-mm KD*P design are its minimum length and the fact that it can be realized with the fewest number of crystals. Both of these factors greatly influence the optical quality and mechanical compactness of the design which were items of consideration under the contract.

2.1.2 Modulator Bandwidth

Referring to Figure 2-1, the modulator cell can be seen to approximate a parallel plate transmission line. Neglecting fringing fields due to edge effects, the distributed capacitance is given by:

$$c' = (K+6)\epsilon_o = 495 \text{ pF/m} \qquad (11)$$

The dielectric constant for KD*P is 50 and the modulator cell consists of 12 percent stray capacity which accounts for the factor (K+6) in Eq. (11). Total capacitance for the 57-mm long cell is 28.5 pF.

TABLE 2-1

ALTERNATE 10-WATT, 100-MHz VIDEO MODULATORS

E/O Crystal	a,b mm	ℓ cm	C pF	R Ω	V Vrms	P Watts	No. Crystals	Remarks
KD*P	1	10.2	48.3	59.4	24.0	10.0	4	
M=2450	3/4	8.0	38.6	74.2	23.0	7.1	4	
K=50	3/4	5.7	27.6	104.0	32.3	10.0	2	Simple Cell
KDP								
M=6280	1	30.2	66.1	43.5	20.8	10.0	8	
K=20	3/4	17.0	38.9	73.6	27.7	10.0	4	
KDA								
M=5300	1	22.2	50.2	57.0	23.9	10.0	12	KDA is difficult to obtain longer than 2 cm
K=21	3/4	13.0	30.7	93.0	30.6	10.0	8	
RDA								
M=4550	1	15.0	31.2	91.8	30.3	10.0	16	RDA is available in sample quantities only to 1 cm length.
K=19	3/4	8.5	18.4	156.0	18.2	10.0	10	

The distributed inductance for the transmission line is given by:

$$L' = \frac{b}{\omega}\,\mu o \qquad (12)$$

where

ω = line width

μo = permeability of free space (1.257 μH/m).

The distributed inductance for the KD*P modulators is 0.375 μH/m.

In the lumped-element center-driven modulator, since the transmission line is not terminated, the applied voltage produces a standing wave as a result of the incident and reflected waves on the line. The phase deviation exhibited by the light-wave traversing the crystal is a function of both the forward and backward traveling waves and can be shown to be given by[5]

$$\Delta\phi = \frac{\pi n^3 r_{63}}{\ell} E_o \cdot \ell \cdot \frac{1}{\sqrt{2}} \sqrt{\left\{\frac{\sin[\omega\ell(n'-n)c]}{\omega\ell(n'-n)c}\right\}^2 + \left\{\frac{\sin[\omega\ell(n'+n)c]}{\omega\ell(n'+n)c}\right\}^2} \qquad (13)$$

where

n = optical index of refraction

ℓ = length of the modulator cell

ω = modulating angular frequency

E_o = electric field of the modulating wave

λ = free space wavelength of the light

n' = modulation index of refraction = $c\sqrt{L'C'}$

r_{63} = electro-optic coefficient.

The modulation efficiency, considering the match in the velocities of the light and the modulation, is defined as:

$$m = \frac{1}{\sqrt{2}} \sqrt{\left\{\frac{\sin[\omega\ell(n'-n)/c}{\omega\ell(n'-n)c}\right\}^2 + \left\{\frac{\sin[\omega\ell(n'+n)c]}{\omega\ell(n'+n)c}\right\}^2} \qquad (14)$$

The bandwidth of the capacitive modulator is determined by the frequency at which the modulation efficiency becomes 0.707. The optical index of refraction of KD*P is 1.512. Substituting values of distributed inductance and capacitance given earlier, we find that the modulation index of refraction is 3.95. Substituting these values into Eq. (14) yields a 70.7 percent modulation efficiency at an operating frequency of 330 MHz. The modulator bandwidth can thus be considered to be 330 MHz.

2.2 BEAM CONDENSER

The laser beam-condenser at the optical input to the modulator is essential when the design employs small cross-section crystals, i.e., 1 mm or less. Without the condenser, the typical laboratory laser beam of 1.4 to 2.0 mm would not fit within the available crystal aperture. Thus, the beam-condenser allows the use of a high aspect ratio modulator with a relatively large laser beam. The beam reduction afforded by the condenser is determined by the ratio of focal lengths of the input and output lenses. The KD*P modulators employ a focal length ratio of 24 mm: 4 mm, and thus reduce input beams by a factor of 6. The condensers provide an input aperture of about 4 1/2 mm.

Laboratory laser beams have Gaussian intensity distributions across their diameter, the latter being specified at the $\left(\frac{1}{\epsilon}\right)^2$ point. Most beams are not collimated but have divergence of the order of a milliradian. Both the laser beam diameter and the beam divergence are important considerations when designing the small cross-section modulator, because the crystal size must be adequate to accommodate the beam spot size throughout the crystal length. Beam divergence becomes an important factor when a condenser is employed, since the condenser magnifies the divergence while reducing the beam. Both effects are governed by the condenser focal length ratio, f_1/f_2.

We now calculate the maximum allowable modulator length for a given crystal cross section, condenser focal length ratio, laser beam spot size and divergence. The maximum length will be set by the distance from the condenser exit lens at which the laser beam has diverged to a diameter equal to the crystal cross section. A focused condenser is assumed; i.e., foci of input and output lenses superimposed. The length limit will be set by other modulator requirements, such as high extinction performance, which may dictate that the modulator exit beam occupy considerably less than all of the crystal cross section.

When a divergent laser beam is used with a modulator employing a beam condenser, the maximum modulator length according to the above constraint is given by:

$$\ell_{max} = \frac{b - \frac{D_1}{f_1/f_2}}{S\left(f_1/f_2\right)\cdot\delta_1} \tag{15}$$

where

b = crystal square cross section

D_1 = laser beam diameter

δ_1 = laser beam divergence

f_1/f_2 = condenser focal length ratio or beam-reduction factor

S = safety factor.

The divergence of the beam in the crystals is given by:

$$\delta_2 = \delta_1\left(f_1/f_2\right) \tag{16}$$

and the spot size at the condenser exit pupil is given by:

$$D_2 = \frac{D_1}{f_1/f_2} \tag{17}$$

Therefore, the beam diverges to fill the crystal cross section, b, in a distance ℓ_{max} when:

$$\ell_{max} = \frac{b - D_2}{\delta_2} \tag{18}$$

When the safety factor, S, is included, Eq. (18) becomes:

$$\ell_{max} = \frac{b - D_2}{S \cdot \delta_2} \tag{19}$$

Equation (18) is plotted in Figure 2-2 for the 2-mm and 1.4-mm beams of the Spectra Physics 125 and 130B lasers. As can be seen from the lower trace, by using a safety factor of 1, the modulator could employ 3/4-mm crystals and be up to 10-cm long and operate with a 2-mm beam of 0.7-mr divergence. The modulator design, represented as a point on the graph, enjoys a safety factor of 1.75 under the 2-mm beam condition, and a safety factor of 2.17 under the 1.4-mm beam condition. These safety factors seemed adequate in view of the 14 dB optical extinction performance achieved (Section 4.1) and the ease of alignment experienced.

Kaminow and Turner have defined a safety factor for the focused beam design.[6] This method does not pass a collimated beam through the modulator cell but instead focuses the beam to a narrow waist at the center of the cell. Unlike the collimated beam design which must consider the beam size and divergence at the exit aperture, the focused beam design must confine the area of interception of both the converging input and diverging output within the crystal aperture. Safety factors of 3 were found required of the focused beam design to ease alignment.

Modulators employing the focused beam design with safety factors near 3 have achieved extinction ratios comparable to the KD*P modulator performance.[7,8] It can be inferred from the comparison of the two beam design conditions that, for equivalent optical extinction ratio performance, a 50 percent drive power

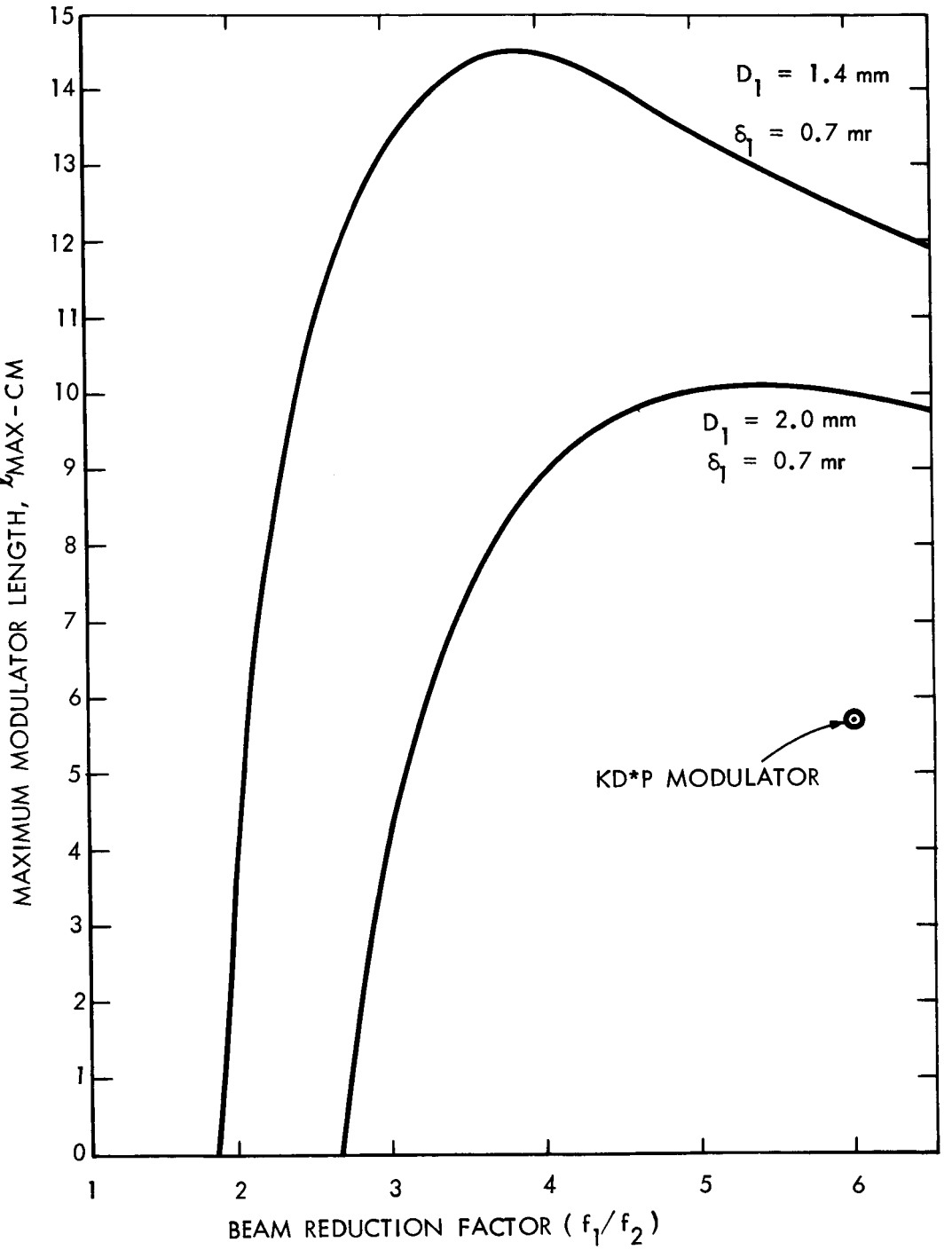

Figure 2-2. Modulator Length vs. Beam Reduction Factor

savings may be afforded by the collimated design because the lower safety factor requirement would allow the use of smaller cross-section crystals.

2.3 CRYSTAL SURFACE QUALITY

An important factor governing modulator performance is crystal optical surface quality. Imperfections on the surface degrade the optical transmission characteristics by scattering the laser beam. High extinction ratio and optical efficiency are dependent upon minimum scattering. Surface defects acting as scattering centers on small cross-section crystals may have a more pronounced effect than the same defects on larger crystals, since they occupy a greater proportion of the crystal aperture.

The discovery of surface defects early in the program initiated an investigation to determine their cause. Crystals pass through three stages of processing before assembly into a modulator: lapp, polish, and antireflection coating. A controlled experiment, where 28 crystals passed through the processing cycle with surface quality measured at each stage, revealed that defects were not due fundamentally to any stage of the cycle. Instead, defects resulted from handling techniques and atmospheric exposure preceding and following these stages.

Surface defects, other than gross physical damage, are of two types: sleeks and blemishes. Figure 2-3 is a micrograph of a 1-mm KDA crystal showing both types. The sleek defect is felt to actually originate as a weakened area during the final strokes of the polish stage. Sleeks are not discernible after polishing but only become defects after considerable exposure to moisture allows the weakened area to etch out. The blemishes on the surface are the result of the crystal having been in contact with crystal debris after the polishing stage, and having been exposed to a moist environment. Crystal debris flakes off the side surfaces when crystals are transported or handled when confined in containers. Upon exposure of the crystal to the atmosphere, debris on the optical surface will rapidly absorb moisture if not immediately removed. Figure 2-4 is included to show the presence of debris and that it can be removed readily. As a result of this investigation processing and handling techniques have been improved and surface defects minimized. Surface quality representative of the crystal shown with debris removed is maintained through the modulator assembly process.

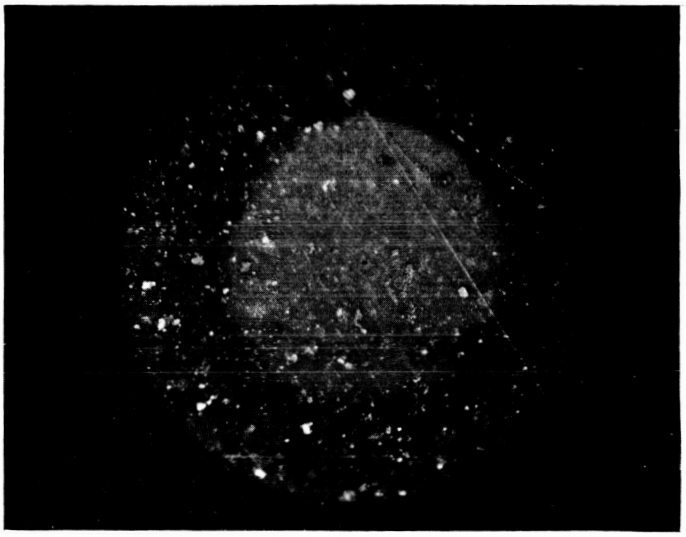

Figure 2-3. Crystal Surface Imperfections

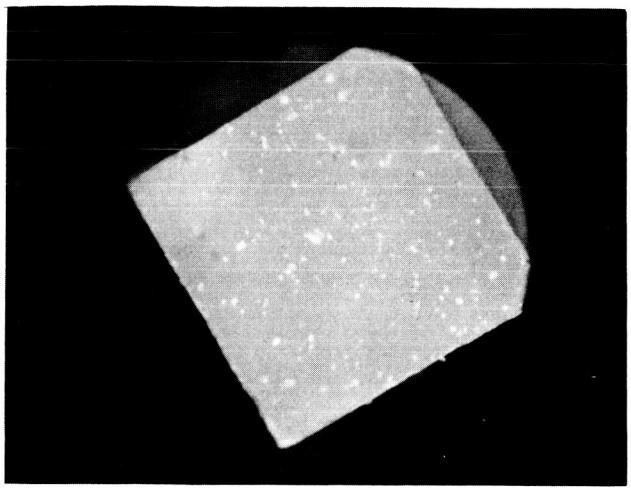

1mm KDA CRYSTAL SHOWING PRESENCE OF DEBRIS

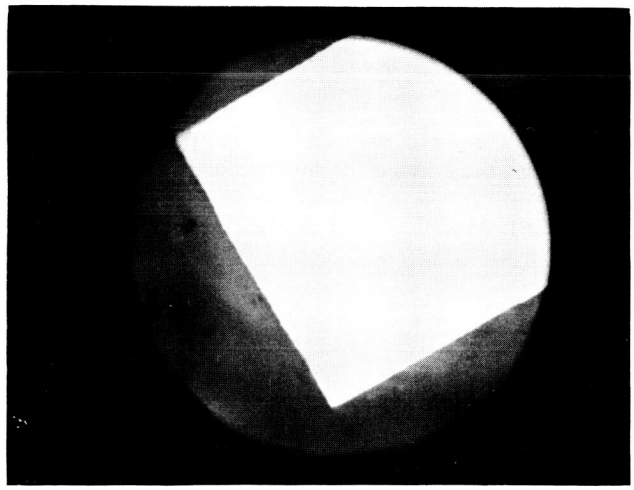

DEBRIS REMOVED

Figure 2-4. KDA Optical Surface Micrographs

SECTION 3

SOLID-STATE DRIVER DESIGN

A 20-watt transistorized distributed amplifier was developed early in the program. Although the device was very useful, allowing us to verify the optical performance of test modulators over the 100-MHz band, it presented difficulty in obtaining any response below about 10 MHz. Additional difficulty in establishing a reasonably flat gain-frequency characteristic led us to abandon the distributed amplifier configuration in favor of a cascade design. The distributed amplifier is treated in more detail in Appendix B. The cascade amplifier developed to solve this 100-kHz to 100-MHz video driver requirement is discussed below.

Figure 3-1 shows the internal view of the solid-state driver that consists of a preamplifier, power amplifier, 40-volt dc power supply, 130-volt dc power supply, and a fan. The construction allows for rack mounting but operation with the optical modulator dictates extremely short cable runs of only a few inches. This limitation will not seriously affect the implementation of the combined modulator and driver into a communication or ranging system, since both amplifiers can be operated remotely from their power supplies. The sizes of the preamplifier and power amplifier are about 1 1/2-inch x 2 1/2-inch x 4 inches and 1 1/2-inch x 2 1/2-inch x 7 inches, respectively, and so lend themselves to compact packaging within the laser head of an optical transmitter.

The preamplifier, Figure 3-2, consists of two Class A common emitter stages, the first employing a type 2N3553 transistor and the second, a 2N3375. Interstage coupling is via a video shunt peaking circuit. The output circuit consists of another shunt peaking circuit. Input and output impedances are 50 ohms. The preamplifier requires a 40-volt power source and provides a nominal 20-dB gain. A 3-dB pad inserted between the preamplifier and the power amplifier affords isolation.

The power amplifier, Figure 3-3, is a two-stage Class A design using the 2N3375 distributed-emitter transistor. Input impedance is 50 ohms. The first stage is an emitter follower used to provide a suitably low output impedance to match the 5-ohm input impedance of the output stage. The output circuit is

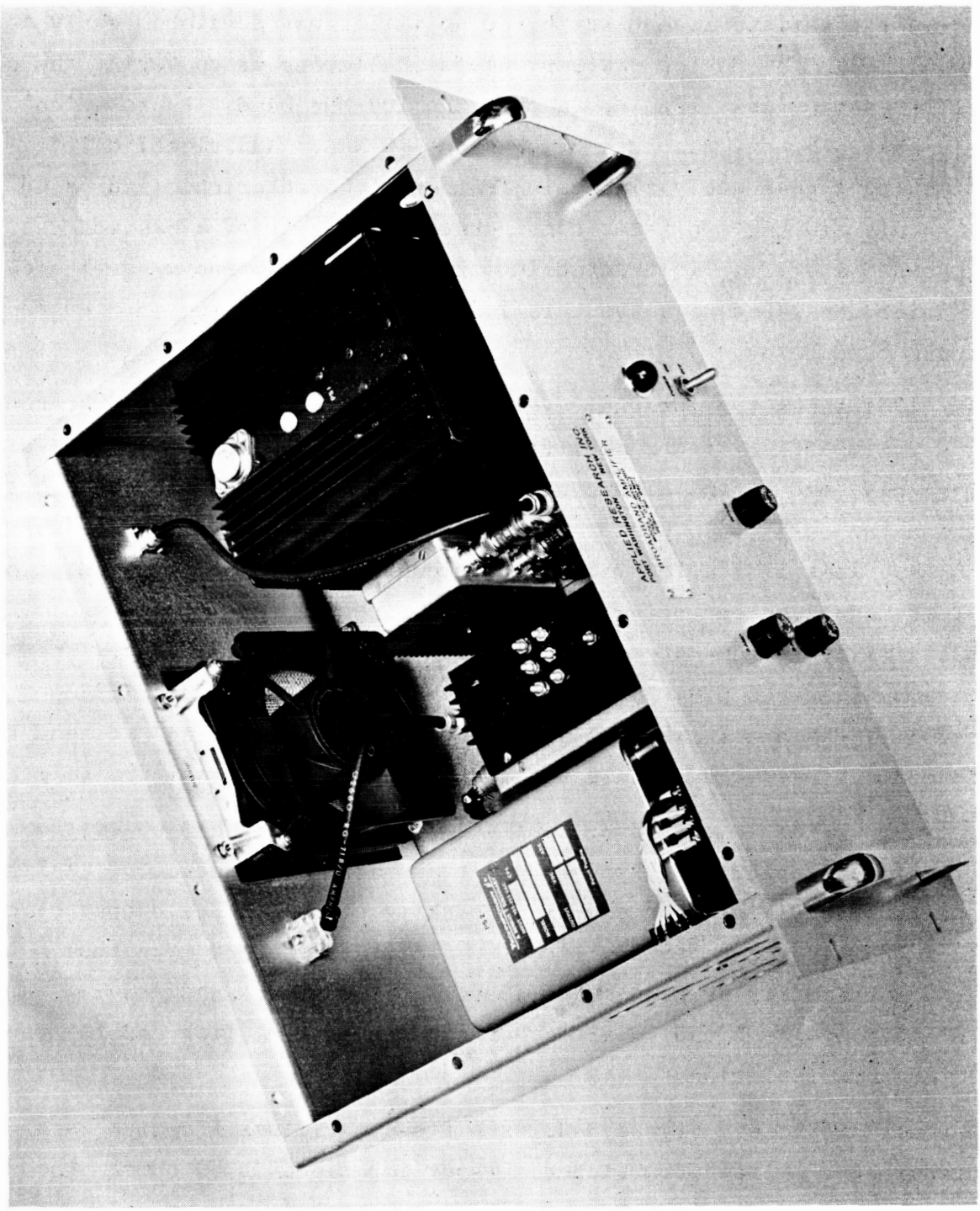

Figure 3-1. 100 MHz Video Amplifier

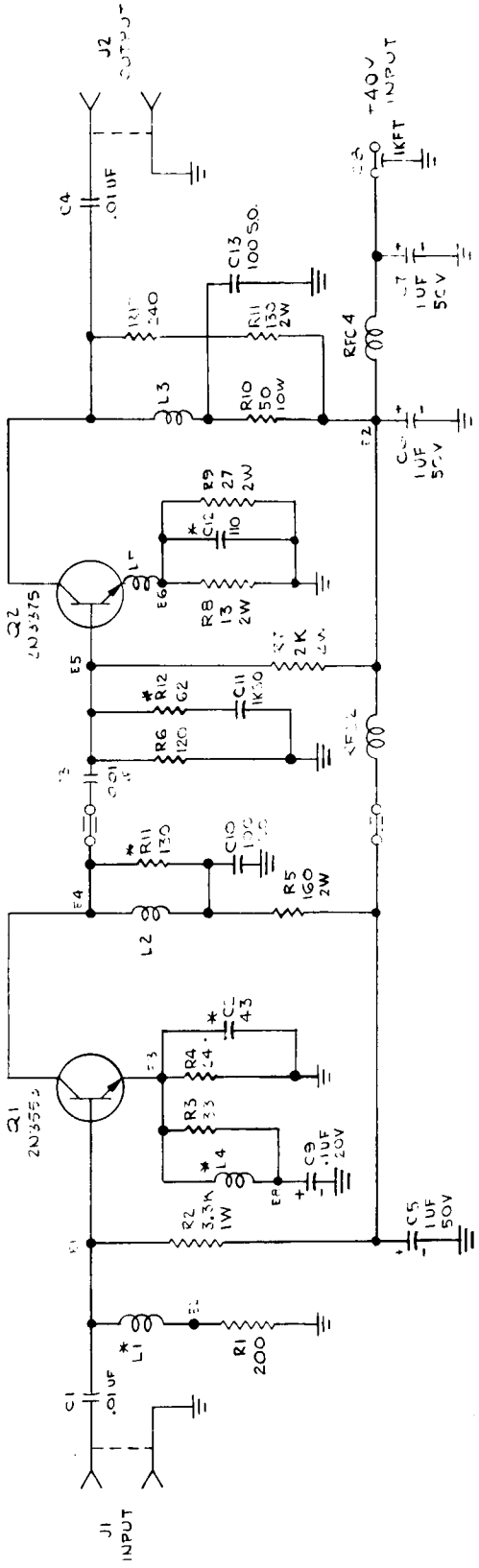

NOTE
1. UNLESS OTHERWISE SPECIFIED.
ALL RES IN Ω ± ½ W
ALL CAP IN MMF
2. * INDICATES NOMINAL VALUE

Figure 3-2. Preamplifier Schematic

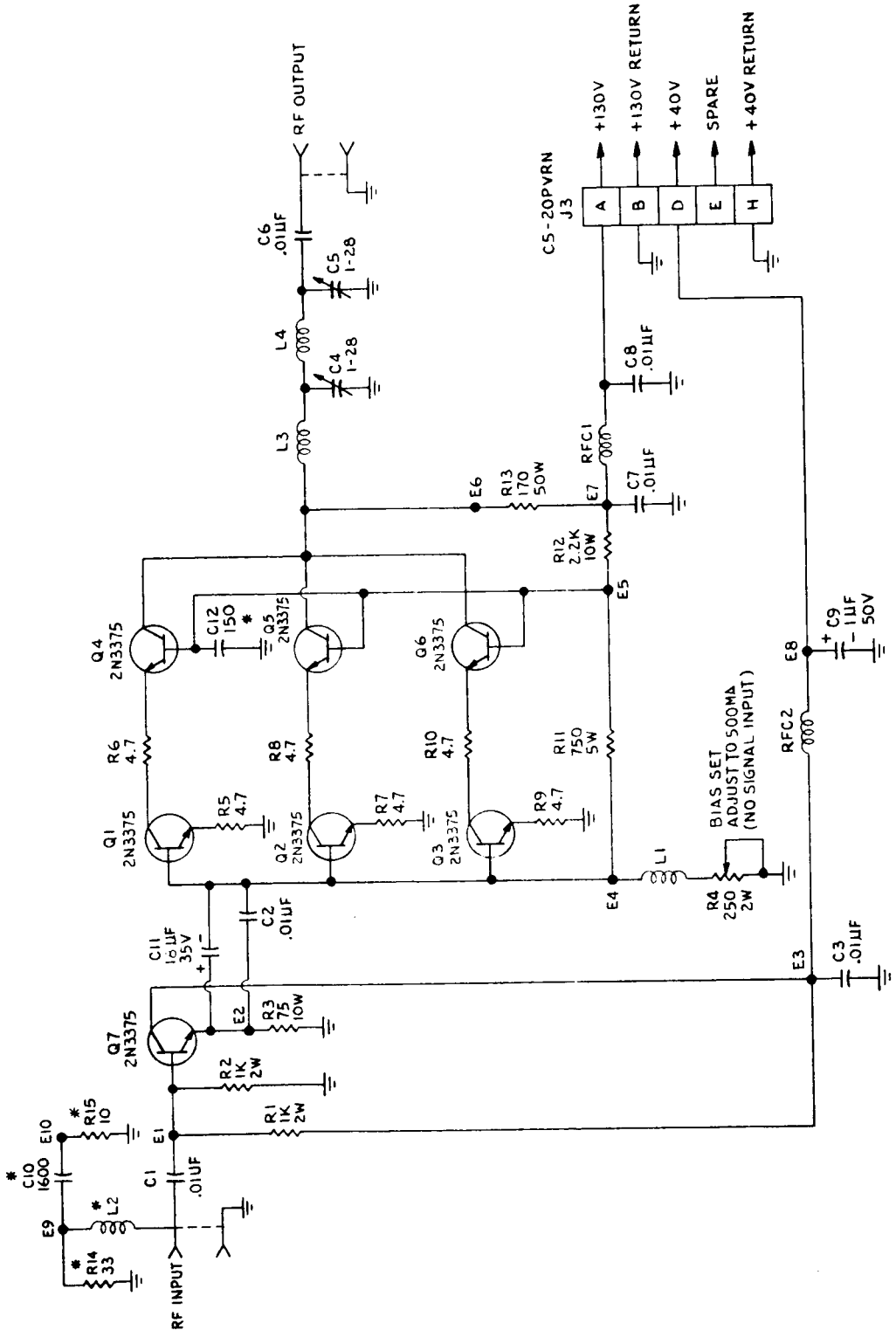

NOTE:
1. UNLESS OTHERWISE SPECIFIED:
   ALL CAPACITOR VALUES ARE IN UUF
   ALL RESISTOR VALUES ARE IN OHMS, 1/2W
2. * INDICATES SELECTED PARTS (NOMINAL VALUES SHOWN)

Figure 3-3. Power Amplifier Schematic

a cascode amplifier. It consists of six transistors arranged in three parallel cascodes, each employing a common emitter driver transistor and a common base output transistor. Terminating collector resistance for the cascode stage is 170 ohms and dissipates the 6-watt maximum signal power when providing the 32-volt rms extinction voltage to the modulator. The output pi network is a wide range matching device that enables the amplifier to achieve a 100-MHz response when driving the modulator and cable capacitance of about 33 pF. Without the matching network, the system could only have achieved the 100-MHz response with a 48-ohm terminating resistance; thus the network provides an equivalent bandwidth improvement factor of 3.5 and corresponding video drive power savings. The power amplifier requires 40-volt dc and 130-volt dc power sources and provides a nominal 15-dB gain.

Both drivers have been used successfully with the optical modulators in broadband tests. Sufficient gain is provided so that the 32-volt rms extinction voltage is developed with only a nominal 0.3-volt drive which is provided by most signal generators. When operating at 91-volt peak-to-peak output, which corresponds to the modulator 32-volt rms extinction voltage requirement, operation over most of the full 100-kHz to 100-MHz band is characterized by less than 5 percent distortion. Figure 3-4 shows the gain-frequency response for the 32-volt output condition.

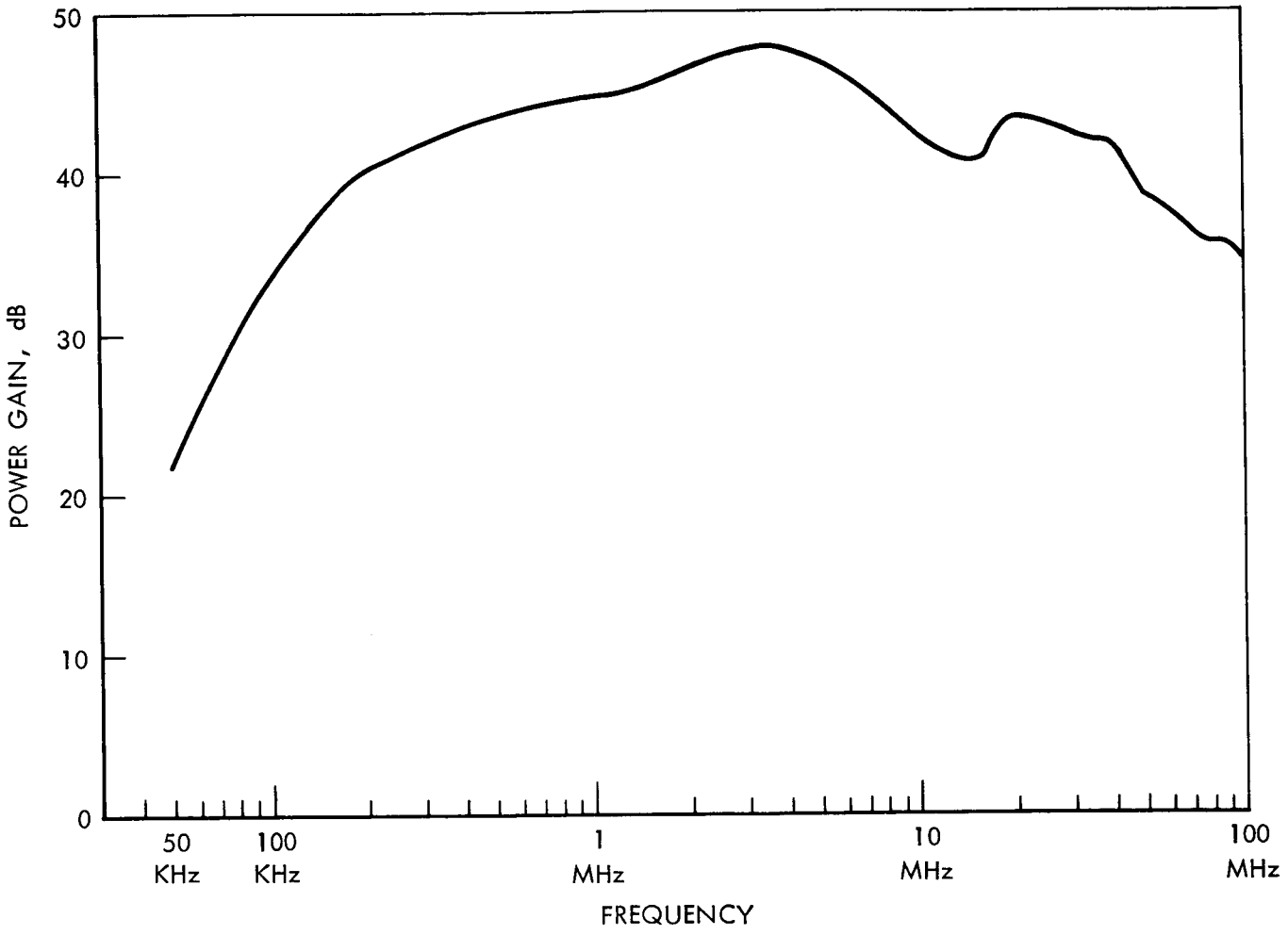

Figure 3-4. 100 MHz Video Amplifier Response

SECTION 4

EXPERIMENTAL

4.1 LOW FREQUENCY TESTS

4.1.1 Extinction Ratio

The extinction ratio is defined as the ratio of the peak-modulated light intensity to the unmodulated light intensity. The extinction ratio, a maximum at a 100 percent modulation level, is the dynamic range of output intensity over which a modulation system is operational. The small cross-section modulators achieved 25:1 (14 dB) power extinction ratios at 100 percent modulation (Figure 4-1). The 32-volt rms drive level for operation to optical extinction agreed with the theoretical value.

4.1.2 Thermal Stability

The modulator, initially at room temperature, was operated in an oven for 2 hours and 22 minutes while a 100-watt heater, placed directly under the modulator, was cycled to maintain the ambient air at +65°C. During this high temperature soak, the modulator underwent a 40°C temperature rise and demonstrated an extinction ratio variation from 25:1 to 14:1. This test pointed out the success of the longitudinal thermal balance design of the modulator. As previously explained in the design discussion, the thermal birefringence of the modulator cell halves is theoretically canceled by employing a half-wave plate at the junction of each cell half, with the sense of their optical axes 180° opposed to each other. The modulator retardation sensitivity to thermal changes corresponding to this measured extinction ratio variation is 0.785 mr/°C.

4.2 OPTICAL EFFICIENCY

Optical efficiency is defined as the ratio of the peak-modulated output light intensity to the input light intensity. Efficiency results obtained by two measurement methods are in close agreement. One method employed optical

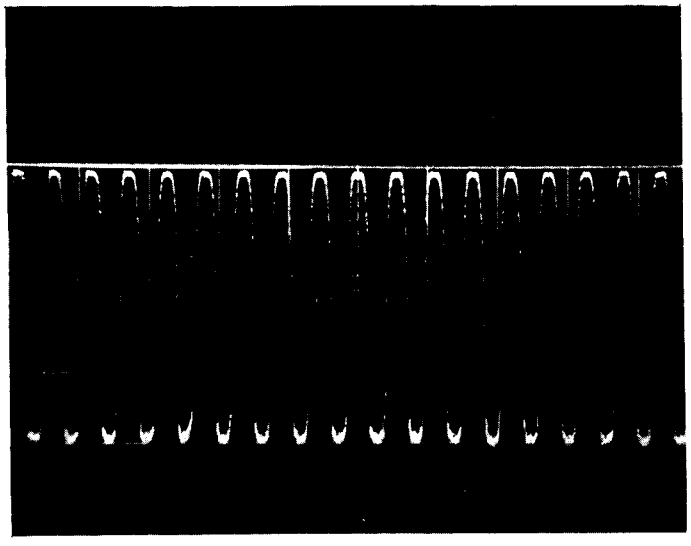

Figure 4-1. KD*P Modulator Extinction Ratio

filters to attenuate the detected laser beam intensity to a level corresponding to the peak-modulated intensity. This method yielded 45 and 36 percent efficiency measurements for modulator S/N -1 and -2, respectively. The second method employed an optical power meter to directly measure the optical transmission of the laser beam through the modulator and its components. This direct measurement method yielded 46.0 and 33.8 percent efficiency values for modulator S/N -1 and -2, respectively. Optical efficiency values for modulator components are given in Table 4-1.

TABLE 4-1

MODULATOR OPTICAL EFFICIENCY

	S/N-1	S/N-2
Beam Condenser	83.3%	83.3%
Modulator Cell	65.7%	53.8%
"Amplitude" Window	84.5%	75.4%
Complete Modulator	46.0%	33.8%

The five individual lenses of the beam condenser combine to present ten air-glass interfaces. Although these surfaces were antireflection coated, the 1 to 2 percent reflection loss per interface accounts for all the beam condenser losses. The complex condenser was dictated by a 4-mm aperture specification that was a contract requirement. Early experiments were conducted with 88 percent efficient condensers providing 3-mm apertures.

Optical losses of the modulator cell are due to reflection and scattering, with the latter predominating. Reflection losses are minimized by constructing a balanced cell with only two crystals with surfaces polished flat to a small fraction of a wavelength and antireflection coated. The scattering is primarily due to the cleaved surfaces of a small cross-section mica waveplate used at the center of the cell. Optical loss of the amplitude window results primarily from absorption in the polarizer.

4.3 SYSTEM OPERATION OVER 100-MHz BANDWIDTH

4.3.1 Direct Detection

The KD*P modulator was operated with the solid-state driver over the 100-kHz to 100-MHz band at 100 percent modulation levels. Direct detection was achieved with a photomultiplier and spectrum analyzer display located within a 120-dB screen room. For a constant 32-volt rms applied to the modulator over the band, the detected amplitude was found to pattern the photomultiplier 100-MHz response and the analyzer gain variation. A more accurate method of determining the presence of 100 percent modulation was required and, consequently, measurements were next performed using the dc shift method.

4.3.2 Modulation Measurements by DC Shift Method

Use of the dc shift method for determination of the modulation level verified the capability of the complete system to develop 100 percent modulation over the 100-kHz to 100-MHz band, with no more than 6-watts video drive power at the modulator. Measurements were extended to 1 kHz by use of a conventional video amplifier verifying the modulator capability to establish optical extinction over the complete 0 - 100-MHz band with a constant 32-volt rms drive voltage. The data points obtained by this method are plotted in Figure 4-2. The accuracy of this method is felt to be $\pm$ 10 percent.

The equipment setup for modulation measurements by the dc shift method is shown in Figure 4-3. The advantage the method offers is that the need for a receiver with high frequency response is eliminated. The laser light is chopped at a 90-Hz rate and, so, the average value of the detected output is easily read on an ac meter. The method involves taking four measurements and is described in the following.

In the internal view of the amplitude modulator (Figure 2-1), the output E vector of the light can be written using Jones Calculus as:

$$\bar{E}_o = \frac{1}{2\sqrt{2}} \begin{bmatrix} e^{jm(t)} & o \\ o & e^{j\gamma_1} \end{bmatrix} \begin{bmatrix} o & 1 \\ 1 & o \end{bmatrix} \begin{bmatrix} e^{-jm(t)} & o \\ o & e^{j\gamma_2} \end{bmatrix} \begin{bmatrix} 1 & -j \\ -j & 1 \end{bmatrix} \begin{bmatrix} 1 & 1 \\ 1 & 1 \end{bmatrix} \bar{E}_i \quad (20)$$

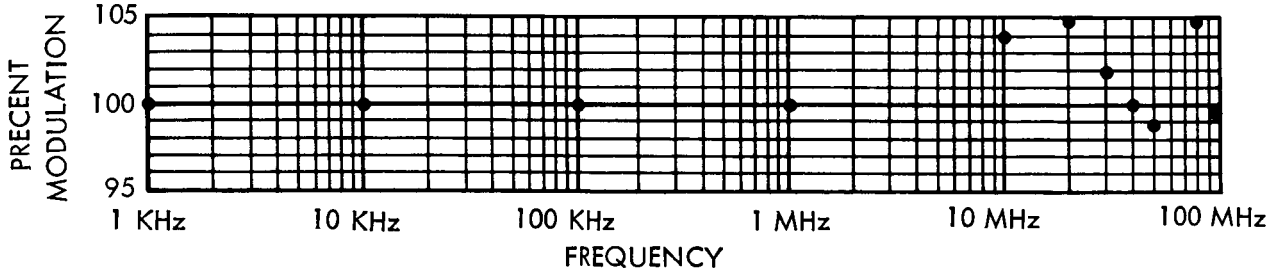

Figure 4-2. Percent Modulation vs. Frequency

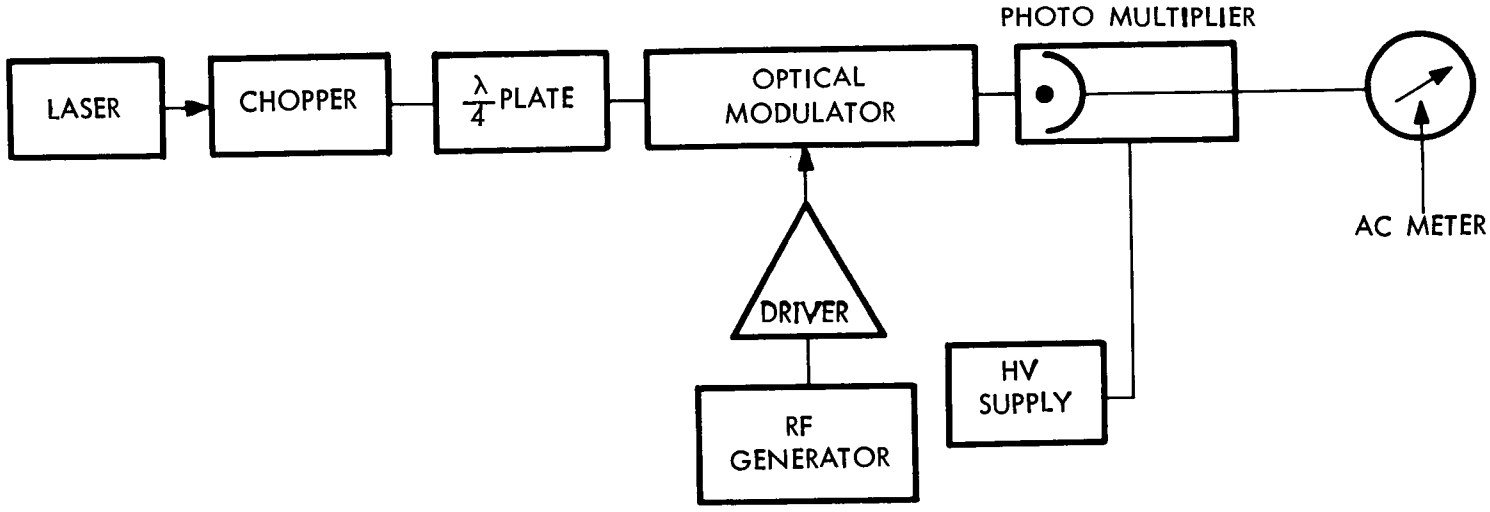

Figure 4-3. Modulation Measurement: DC Shift Method

where

$\bar{E}_i$ = input E vector

$m(t) = \Gamma \sin \omega_m t$

Γ = effective peak phase retardation

ω_m = modulating frequency

γ_1, γ_2 = net phase retardation of one component relative to the other due to natural birefringence.

The peak phase shift, Γ, has been given in Eq. (1) in terms of the electro-optic material parameters with the drive peak voltage equal to the half-wave retardation voltage. The right-hand side of Eq. (20) consists of Jones matrices for crystal 1, half-wave plate, crystal 2, quarter-wave plate and polarizer, respectively. Because of the axis reversal of crystal 2, the phase shift of the x component is reversed in sign, while the natural birefringence effect remains the same as crystal 1. As will be evident in the following analysis, such an arrangement tends to offset the effect of natural birefringence of one crystal with that of the other.

Inserting the Jones matrix for the input E vector, the output E vector is:

$$E_1 = \frac{1}{2\sqrt{2}} \begin{bmatrix} 1 & 1 \\ 1 & 1 \end{bmatrix} \begin{bmatrix} e^{jm(t)} & o \\ o & e^{j\gamma_1} \end{bmatrix} \begin{bmatrix} o & 1 \\ 1 & o \end{bmatrix} \begin{bmatrix} e^{-jm(t)} & o \\ o & e^{j\gamma_2} \end{bmatrix} \begin{bmatrix} 1 & -j \\ -j & 1 \end{bmatrix} \begin{bmatrix} 1 \\ 1 \end{bmatrix} \tag{21}$$

With external optical biasing, the output E vector is:

$$E_2 = \frac{1}{2} \begin{bmatrix} 1 & 1 \\ 1 & 1 \end{bmatrix} \begin{bmatrix} e^{jm(t)} & o \\ o & e^{j\gamma_1} \end{bmatrix} \begin{bmatrix} o & 1 \\ 1 & o \end{bmatrix} \begin{bmatrix} e^{-jm(t)} & o \\ o & e^{j\gamma_2} \end{bmatrix} \begin{bmatrix} 1 \\ 1 \end{bmatrix} \tag{22}$$

The magnitudes of the output light intensities are obtained by multiplying out the above two equations and taking the magnitude-squares:

$$S_1^+ = k_1\left\{1 + \text{Cos}\left(2\ \Gamma\ \text{Sin}\omega_m t + 2\delta\right)\right\} \tag{23}$$

$$S_2^+ = k_2\left\{1 + \text{Sin}\left(2\ \Gamma\ \text{Sin}\omega_m t + 2\delta\right)\right\} \tag{24}$$

where

$$2\delta = \gamma_1 - \gamma_2 \tag{25}$$

Equations (23 and (24) can be expanded out in their trigonometric identities and then in Bessel functions. Retaining only the dc terms after the expansions, one obtains

$$S_1 = k_1\left[1 + J_o(2\Gamma)\,\text{Cos}\ 2\delta\right] \tag{26}$$

$$S_2 = k_2\left[1 + J_o(2\Gamma)\,\text{Sin}\ 2\delta\right] \tag{27}$$

For both measurement conditions, without (1) and with (2) external optical biasing, two measurements are taken corresponding to the presence (m) and absence (n) of the 100 percent modulation drive voltage. Thus, the four results obtained for the four distinct measurements allow the determination of the four unknowns, k_1, k_2, Γ, and δ.

$$S_1^m = k_1\left[1 + J_o(2\Gamma)\,\text{Cos}\ 2\delta\right] \tag{28}$$

$$S_1^n = k_1\left[1 + 1\right] = 2k \tag{29}$$

$$S_2^m = k_2\left[1 + J_o(2\Gamma)\,\mathrm{Sin}\ 2\delta\right] \tag{30}$$

$$S_2^n = k_2\left[1 + 0\right] = k_2 \tag{31}$$

Combining Eqs. (28) - (31) and rearranging, we obtain

$$J_o(2\Gamma) = \sqrt{\left(\frac{2S_1^m}{S_1^n} - 1\right)^2 + \left(\frac{S_2^m}{S_2^n} - 1\right)^2} \tag{32}$$

and

$$2\delta = \tan^{-1}\left[\frac{\left(\frac{S_2^m}{S_2^n} - 1\right)}{\left(\frac{2S_1^m}{S_1^n} - 1\right)}\right] \tag{33}$$

The percentage amplitude modulation is given in terms of the peak phase retardation by:

$$AM = 100\ \mathrm{Sin}(2\Gamma)\ \text{percent} \tag{34}$$

4.4 MODULATOR SYSTEM PULSE PERFORMANCE

The KD*P modulator was operated with a pulse modulation format at PRF's up to 10-MHz. The pulse source was a Tektronix Programable Pulse Generator that provided a 10-volt pulse amplitude enabling the modulator to establish 17.5 percent optical intensity modulation. Operation at higher PRF's was limited by the generator. Figure 4-4 shows both the drive pulse and the detected output of a photomultiplier with the system operating at 1-MHz PRF.

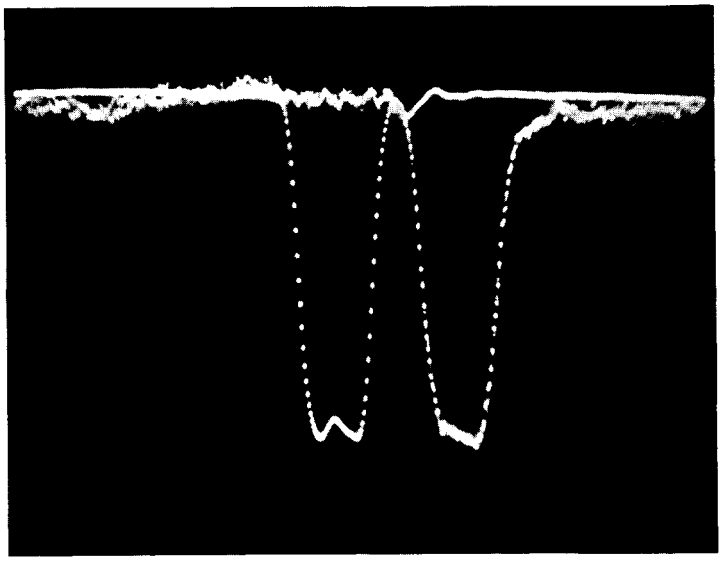

MODULATOR PULSE RESPONSE

PRF 1 MHz, WIDTH 50 ns

MODULATOR INPUT RISE TIME 10 ns

DETECTED OUTPUT RISE TIME 12 ns

Figure 4-4. Modulator Pulse Response

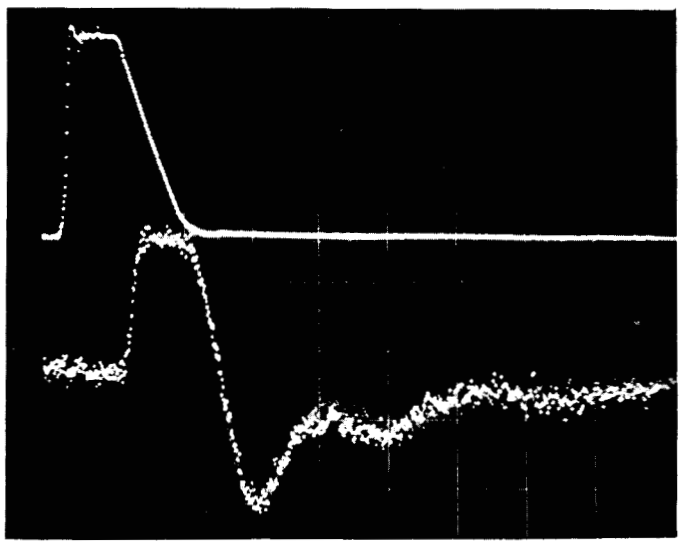

PRF 2.5 MHz, WIDTH 75 ns

Figure 4-5. Modulator System Pulse Response

The apparent lack of coincidence between the pulses is due to synchronization limitations of the dual beam sampling oscilloscope used. The 2-ns degradation to the 10-ns input pulse rise time is attributable entirely to the response of the photomultiplier. The 330-MHz modulator bandwidth would degrade a unit step input to an optical pulse rise time of about 1.0 nanosecond as a first order approximation.[3] The modulator itself is theoretically capable of operation at PRF's of a few hundred megahertz and at 100 percent modulation levels.

The modulator was operated with the 6-watt drive amplifier under pulsed conditions again up to 10-MHz PRF's but near 100 percent modulation levels. Although the amplifier was not designed for pulse applications, the response as seen in Figure 4-5 is satisfactory for many PCM communication applications. The upper trace shows the 75-ns pulsewidth, 2.5-MHz PRF input pulse chain to the driver; the lower trace shows the detected output. Input 10-ns rise time is detected as having been degraded to 14 ns.

4.5 DESIGN AND TEST DATA SUMMARY

The pertinent design characteristics and experimental test results for the small cross-section KD*P modulator are presented in Table 4-2.

TABLE 4-2

KD*P MODULATOR SUMMARY

Cell Length (ℓ)	57 mm	Modulator Bandwidth	330 MHz
Cross-Section (b)	3/4 mm	Extinction Ratio	25:1
Aspect Ratio (ℓ/2)	76	Optical Efficiency	~ 45 %
Extinction Voltage	32 Vrms	Thermal Stability	0.785 mr/^{o}C
Capacitance	28.5 pF	Aperture	4 1/2 mm
Drive Power	60 mW/MHz	Wavelength	6328 $\pm$50 $\mathring{A}$

SECTION 5

CONCLUSIONS

The project goals of providing two working 100-MHz video bandwidth modulators and solid-state drivers were achieved. The modulators provide 100 percent optical intensity modulation over the 100-MHz bandwidth when operated at 32-volts rms. Modulator capacitance was minimized enabling a transistorized amplifier to provide the 32-volt modulation signal over the band when terminated with a resistive load dissipating 6 watts. The modulation system thus achieved a drive power requirement of 60 milliwatts per megahertz of operating bandwidth. This represents a significant advance in the state-of-the-art of capacitive modulators; previous devices such as the S2A required some 5 watts/MHz and operated at 500-volts rms--a level incompatible for broadband operation with transistorized drivers.

The modulators provided a 25:1 optical extinction ratio when operated with a 1.4-mm diameter Gaussian beam. This performance is comparable to that of the S2A and, in general, exceeds the dynamic range requirements for many communication applications. The KD*P modulator was optimized for operation at 6328 $\pm$50 Å; however, it can be provided to operate at any wavelength within the spectral transmission region of KD*P, 0.4 to 1.2 microns.

The CW modulation tests and the pulse response measurements show the feasibility of employing the modulator in either CW or PCM communications systems. The compact size and termperature independent performance of the high aspect ratio, KD*P modulator indicate feasibility for future use of similar designs in broadband space communication systems.

A space qualification design and test effort must be carried out before implementing the space modulation system with the low drive power modulator. The temperature independent performance demonstrated at atmospheric pressure must be verified in the vacuum of space. A space qualification program would logically include consideration of the active electro-optic elements, lithium niobate and tantalate. Although these elements promise a drive power requirement an order of magnitude below that of KD*P (see Appendix A), the present

laser-induced distortion and the large temperature dependent birefringence may preclude their eventual use in systems using high power lasers or those exposed to large temperature changes.[1,2]

Two modulator performance characteristics important to the space communication application are optical efficiency and phase front distortion. Optical efficiency must be increased. Modulator output phase front distortion is presently unknown; studies indicate phase distortion substantially less than a fraction of a wave will be required for deep-space communicaton.

SECTION 6

REFERENCES

1. A. Ashkin et al., "Optically-Induced Refractive Index Inhomogeneities in $LiTaO_3$," Applied Phys. Letters, vol.9, pp. 72-74; 1 July 1966.

2. E. G. Spencer and P. V. Lenzo, "Lithium Niobate and Lithium Tantalate in Electro-Optic Device Applications," NEREM Record, pp. 230-231; 1966.

3. Millman and Taub, Pulse and Digital Circuits.

4. "Proposal for Development of a Wide-Band High Efficiency Optical Modulator," ARL, no. B-85-65; 3 December 1965.

5. C. J. Peters, "Gigacycle-Bandwidth Coherent-Light Traveling-Wave Amplitude Modulator," Proc. IEEE, vol. 53, no. 5, pp. 455-460; May 1965.

6. I. P. Kaminow and E. H. Turner, "Electro-optic Light Modulators," Applied Optics, vol. 5, no. 10, pp. 1612-1628; October 1966.

7. R. T. Denton et al., "Lithium Tantalate Light Modulators," J. Appl. Phys, to be published.

8. R. T. Denton, T. S. Kinsel, and F. S. Chen, "225 Mc/s Optical Pulse Code Modulator," Proc. IEEE (Letters), vol. 54, no. 10, pp. 1472-1473; October 1966.

APPENDIX A

EXPERIMENTAL TEST MODULATORS

Experimental test modulators constructed early in the program used 1-mm square cross-section crystals of KDA (potassium dihydrogen arsenate) and LN (lithium niobate) in balanced cells of 37-mm and 40-mm length, respectively. These devices employed laser beam condensers providing an input aperture of about 2-2/3 mm. The modulators were constructed to determine the feasibility of employing beam condensing optics in conjunction with small cross-section crystals so as to reduce modulator video drive power requirements while simultaneously allowing the use of large diameter laser beams.

KDA TEST MODULATOR

A test modulator, Figure A-1, assembled with a balanced two crystal polarization modulator cell of KDA achieved an extinction ratio of 32:1, an optical efficiency of 43 percent, and a 100 percent modulation voltage of 143-volts rms. The latter agreed exactly with that predicted by the half-wave field distance product for KDA and the aspect ratio of the modulator cell.

The KDA modulator was operated at modulation rates up to 100 MHz and levels up to 60 percent for prolonged periods without any discernible performance degradation. Extinction ratio and modulation sensitivity were unaffected by the RF exposure. Figure A-2 shows 10-MHz modulation detected at a 60 percent modulation level superimposed on a chopped light waveform and the corresponding 70.7-volt drive. Broadband operation at a 100 percent modulation level was prevented due to lack of a suitable driver.

Capacitance measurements agreed with theoretical values for the KDA assembly. Of the total 9.7 pF presented by the balanced modulator, 7.0 pF were attributable to the KDA crystal. The modulator possessed 28 percent stray capacitance.

Performance results for the KDA polarization modulator are shown in Table A-1. The 333-mW/MHz drive power requirement is based upon a 3.5 load improvement factor found to be feasible as demonstrated by the 100-MHz amplifier delivered under this contract.

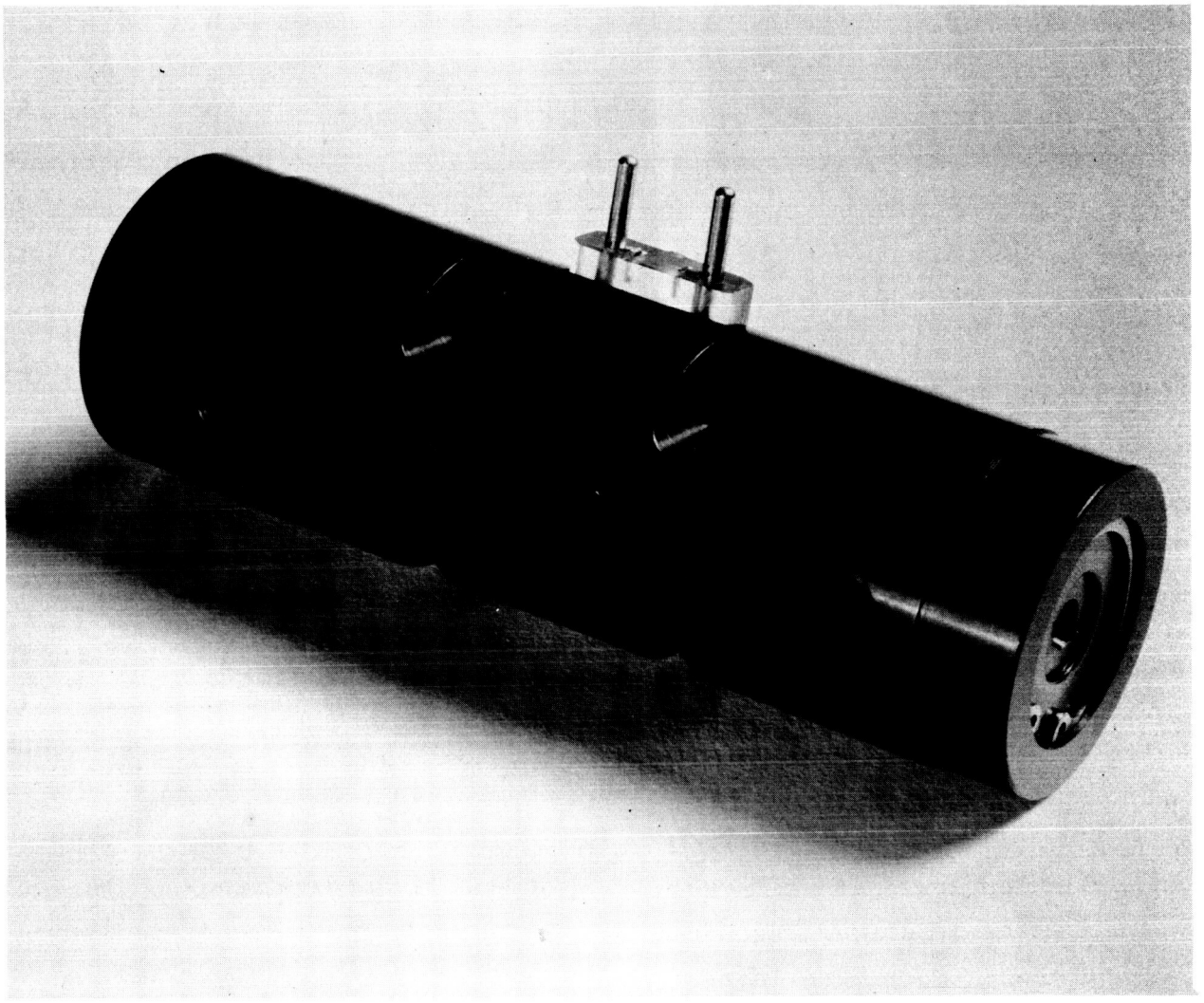

Figure A-1. Test Modulator

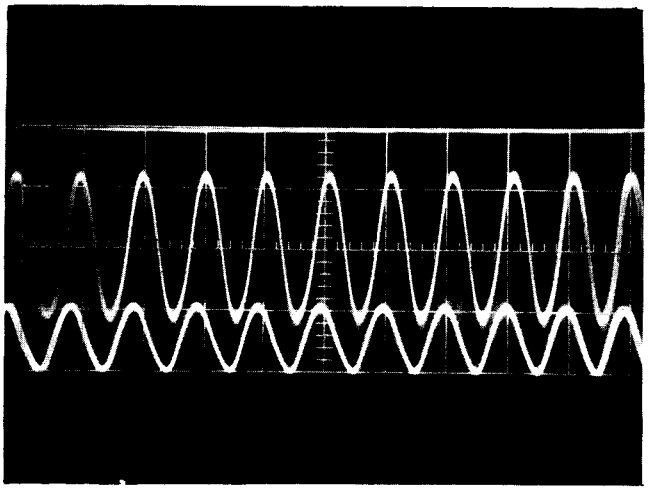

Upper: 60% Modulated-Chopped Light.
Lower: 200 Volt Peak-to-Peak Drive Voltage.

Figure A-2. KDA Modulator Operation at 10 MHz

TABLE A-1

KDA TEST MODULATOR SUMMARY

Cell Length (ℓ)	37-mm	Extinction Ratio	32:1
Cross-Section (b)	1-mm	Optical Efficiency	43%
Aspect Ratio (ℓ/b)	37	Extinction Voltage	143 V rms
Aperture (nom)	2 2/3-mm	Capacitance	9.7 pF
Modulator Length	4.625 in.	Modulator Bandwidth	1045 MHz
Modulator Diameter	1.50 in.	Drive Power	333 mW/MHz

LN TEST MODULATOR

A test modulator was assembled with a balanced four-crystal polarization modulator cell of the ferroelectric LN with a square 1-mm cross section and 40-mm length. The half-wave retardation voltage for LN is 1040-volts rms, thus enabling this test modulator with aspect ratio of 40 to operate to extinction with 26-volts rms drive voltage. Agreement between the predicted and measured extinction voltage was obtained only after both the crystal electrode surfaces and the electrodes themselves were plated. Prior to plating, a 100 percent modulation drive voltage of 67 volts was required.

Extinction ratio performance of the LN modulator was poor. Operating with the 1.4-mm beam of the Spectra Physics 130B laser, a 4.9:1 extinction ratio was attained. A major factor contributing to the poor extinction may have been due to scattering within the crystals. Some evidence of internal inhomogeneities was found upon microscopic investigation of the LN optical surfaces. Micrographs in Figure A-3 reveal these inhomogeneities as dark patches. Detailed investigation showed that abrupt discontinuities in the index of refraction were discernible throughout the full length of most of the LN crystals.

A seventeen-hour continuous exposure to a 50-mW laser beam was attended with a 10 percent decrease in extinction ratio performance and a lesser decrease in optical efficiency. These results do not conclusively show direct evidence of the damageability of LN as the variations are within measurement accuracy and alignment stability. Reoperation with the 1-mW laser beam one week later demonstrated the original 4.9:1 extinction ratio.

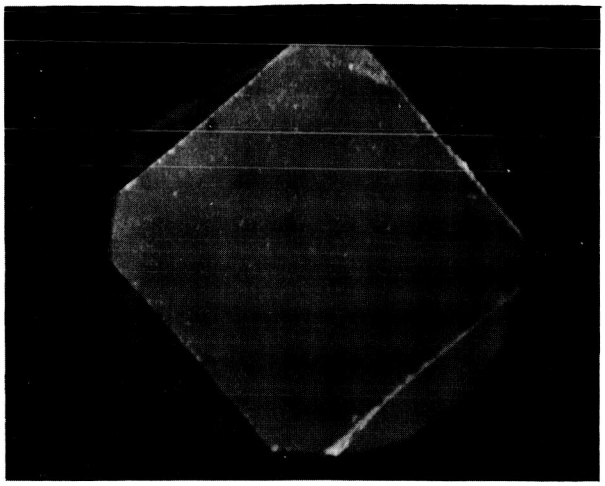

LN INTERNAL INHOMOGENEITIES

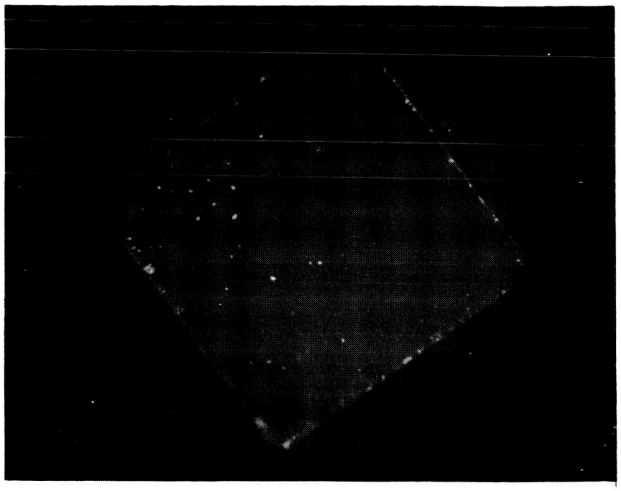

SURFACE DEBRIS AND NEAR-SURFACE "FROSTING"

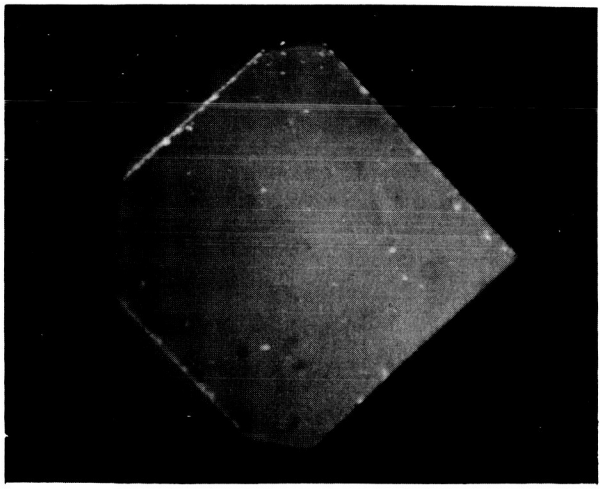

LN INTERNAL INHOMOGENEITIES

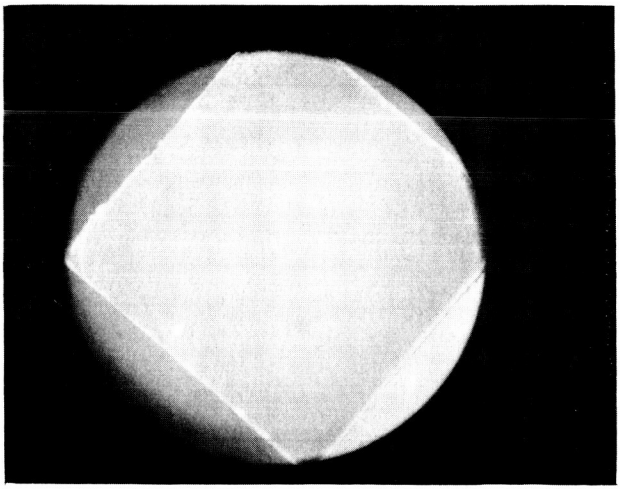

LN HIGH POLISH QUALITY

Figure A-3. LN Optical Surface Micrographs

The optical efficiency of the LN modulator was 28 percent, a value considerably lower than that of the KDA unit because of the internal scattering losses of our samples of LN. Table A-2 summarizes the performance characteristics of the LN polarization modulator.

TABLE A-2

LN TEST MODULATOR SUMMARY

Cell Length (ℓ)	40-mm	Extinction Ratio	4.9:1
Cross-Section (b)	1-mm	Optical Efficiency	28%
Aspect Ratio (ℓ/b)	40	Extinction Voltage	26 V rms
Aperture (nominal)	2-2/3-mm	Capacitance	13.8 pF
Modulator Length	4.625 in.	Modulator Bandwidth	1310 MHz
Modulator Diameter	1.50 in.	Drive Power	13.9 mW/MHz

The product of permittivity and megahertz has been suggested as a figure of merit for electro-optic crystal materials, as it is directly proportional to the drive power requirement per unit operating bandwidth per unit modulator cell length for a given aspect ratio.[7] M is the rms value of the half-wave retardation voltage and is given by

$$M = \frac{\{E \cdot \ell\}_{\lambda/2}}{2\sqrt{2}} = \frac{\lambda}{2\sqrt{2}\, n_o^3 r_{63}} \tag{35}$$

The figure of merit in joules per meter is given by:

$$K\epsilon_o M^2 = \frac{P(\ell/b)^2}{2\pi f_2 \ell} \tag{36}$$

or

$$K\epsilon_o M^2 = \frac{P \cdot \ell}{2\pi f_2 b^2} \tag{37}$$

A comparison of the figure of merit and other electro-optic crystal characteristics is given in Table A-3. The exceptionally low figure of merit for LN indicates a tenfold savings in drive power over the KD*P modulators supplied under this contract that achieved a 60-mW per MHz drive requirement. LN also is hard, non-hygroscopic, and is easily polished to high optical surface quality. Despite these advantages, the poor extinction ratio performance and excessive scattering losses experienced with the LN samples which we tested and believe to be representative of what is readily available today, precluded our selection of LN as a material for use in the deliverable units.[1,2]

TABLE A-3

ELECTRO-OPTIC CRYSTAL CONSTANTS

Xtal	r_{63}(m/v)	η_o	η_e	K	tan δ	η_o^3	M(vrms)	$(E.\ell)_{\lambda/2}$	$K\epsilon_o M^2$ joules/meter
KDP	$10.3\left(10^{-12}\right)$	1.512	1.47	20.2	$5\left(10^{-4}\right)$	3.45	6280	17750.	$7060\left(10^{-6}\right)$
KD*P	$26.4\left(10^{-12}\right)$	1.512		50.		3.45	2450	6940.	$2658\left(10^{-6}\right)$
KDA	$10.9\left(10^{-12}\right)$	1.5707	1.5206	21.0	$\sim 10\left(10^{-4}\right)$	3.87	5300	15000.	$5215\left(10^{-6}\right)$
ADP	$4.9\left(10^{-12}\right)$	1.525	1.479	14.3	$5\left(10^{-4}\right)$	3.54	12880	36430.	$21000\left(10^{-6}\right)$
ADA	$5.5\left(10^{-12}\right)$	1.5766	1.5217	14.0	$\sim 10\left(10^{-4}\right)$	3.91	10380	29370.	$13350\left(10^{-6}\right)$
RDP	$11.0\left(10^{-12}\right)$	1.52		15.		3.51	5780	16330.	$4440\left(10^{-6}\right)$
RDA	$13.0\left(10^{-12}\right)$	1.559	1.520	19.	$\sim 10\left(10^{-4}\right)$	3.78	4550	12860.	$3480\left(10^{-6}\right)$
LN		2.286	2.200	28.			1040	2940.	$265\left(10^{-6}\right)$
KTN				28.4			3535	10000.	$3145\left(10^{-6}\right)$
LT		2.175	2.180	43			1004	2840.	$383\left(10^{-6}\right)$

APPENDIX B

20 WATT TRANSISTORIZED DISTRIBUTED AMPLIFIER

A transistorized distributed amplifier system was designed to provide a 100-volt peak-to-peak output signal over a 100-MHz video bandwidth when operated in conjunction with capacitive loads presented by the optical modulator. The characteristic impedance of the output transmission line was 50 ohms and when terminated with a matched load the amplifier delivered 20 watts of signal power. The amplifier system comprised three separate amplifying units (Figure B-1).

The system operated to full output developing 23 dB of power gain when driven with a nominal 100 mW. The first and second preamplifiers developed 13 dB of power gain. The high power unit employed the 2N3375 in eight stages and developed 10 dB of power gain.

Substantial use of the distributed amplifer was made during broadband modulation experiments conducted with the KDA and LN test modulators. The output voltage swing was raised to 200-volts peak-to-peak by a bifilar wound ferrite auto-transformer for application with the KDA modulator (Figure A-2).

Two characteristics of this amplifier design were the fundamental reasons for abandoning it in favor of a cascade amplifier as the solution to the 100-MHz video bandwidth requirement. It was very difficult by tuning to extend the low frequency response substantially below a few megahertz. Furthermore, the gain characteristic varied by several decibel over the band, making pre-emphasis of the input signal a necessity for any wideband communication application requiring a 100-MHz instantaneous bandwidth. Despite these characteristics the distributed amplifier would be quite satisfactory as a driver where fixed frequencies are involved such as in multiple-tone ranging systems and subcarrier communication systems. A third argument favoring the cascade amplifier was that our experience had indicated it would be a less complicated and smaller device thus offering system packaging advantages.

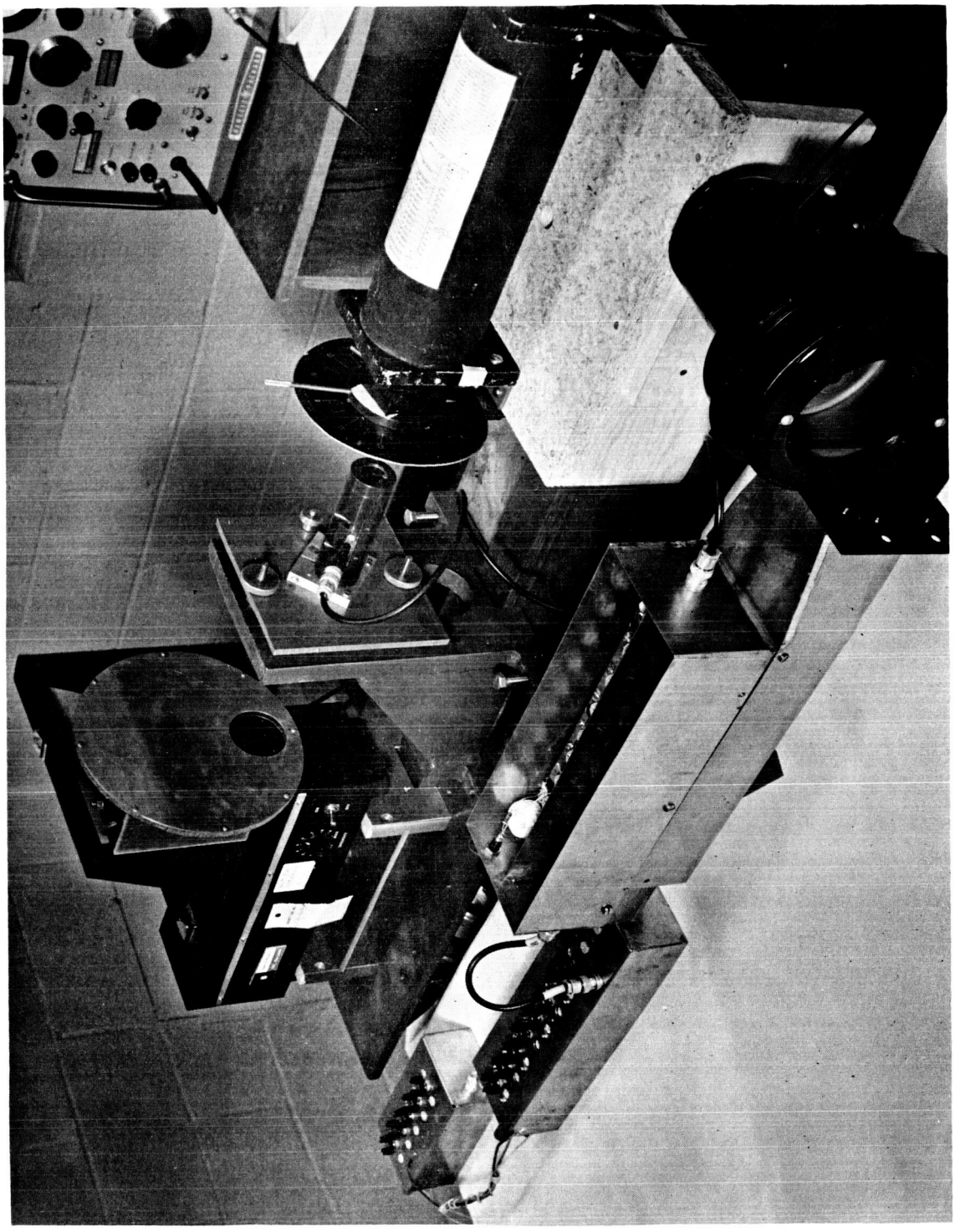

Figure B-1. 20 Watt Transistorized Distributed Amplifier